Appl Biochem Biotechnol (2011) 165:426–441
DOI 10.1007/s12010-011-9262-7

Effect of Internal Diffusional Restrictions on the Hydrolysis of Penicillin G: Reactor Performance and Specific Productivity of 6-APA with Immobilized Penicillin Acylase

Pedro Valencia · Sebastián Flores · Lorena Wilson · Andrés Illanes

Received: 26 October 2010 / Accepted: 4 April 2011 /
Published online: 20 April 2011

Abstract A mathematical model that describes the heterogeneous reaction–diffusion process involved in penicillin G hydrolysis in a batch reactor with immobilized penicillin G acylase is presented. The reaction system includes the bulk liquid phase containing the dissolved substrate (and products) and the solid biocatalyst phase represented by glyoxyl-agarose spherical porous particles carrying the enzyme. The equations consider reaction and diffusion components that are presented in dimensionless form. This is a complex reaction system in which both products of reaction and the substrate itself are inhibitors. The simulation of a batch reactor performance with immobilized penicillin G acylase is presented and discussed for the internal diffusional restrictions impact on effectiveness and productivity. Increasing internal diffusional restrictions, through increasing catalyst particle size and enzyme loading, causes impaired catalyst efficiency expressed in a reduction of effectiveness factor and specific productivity. High penicillin G initial concentrations decrease the impact of internal diffusional restrictions by increasing the mass transfer towards porous catalyst until product inhibition becomes significant over approximately 50 mM of initial penicillin G, where a drop in conversion rate and a maximum in specific productivity are then obtained. Results highlight the relevance of considering internal diffusional restrictions, reactor performance, and productivity analysis for proper catalyst and reactor design.

P. Valencia (✉)
Department of Chemical and Environmental Engineering, Universidad Técnica Federico Santa María,
PO Box 110-V, Valparaíso, Chile
e-mail: pedro.valencia@usm.cl

L. Wilson · A. Illanes
School of Biochemical Engineering, Pontificia Universidad Católica de Valparaíso, P.O. Box 4059,
Valparaíso, Chile

A. Illanes
e-mail: aillanes@ucv.cl

S. Flores
Center for Mathematical Modeling, Universidad de Chile, Santiago, Chile

Keywords Heterogeneous biocatalysis · Immobilized enzyme · Penicillin acylase · Penicillin G · Enzyme reactor · Diffusional restrictions

Nomenclature

A	Total catalyst surface area
D_e	Penicillin G effective diffusion coefficient
D_{e1}	PAA-effective diffusion coefficient
D_{e2}	APA-effective diffusion coefficient
E	Catalyst enzyme concentration
E_R	Reactor enzyme concentration
k	Reaction rate constant
K	Michaelis constant for penicillin G
K_1	Competitive product inhibition constant for PAA
K_2	Non-competitive product inhibition constant for APA
K_S	Uncompetitive inhibition constant for penicillin G
p	Dimensionless PAA concentration
P_1	PAA concentration
P_{1b}	Bulk PAA concentration
P_2	APA concentration
P_{2b}	Bulk APA concentration
q	Dimensionless APA concentration
Q_p	Volumetric productivity
Q_{pe}	Specific productivity
r	Variable radius inside the catalyst particle
R	Catalyst particle radius
S	Substrate concentration inside catalyst
s	Dimensionless substrate concentration
S_b	Bulk substrate concentration
S_{b0}	Initial bulk substrate concentration
t	Reaction time
T	Characteristic time (R^2/D_e)
v	Reaction rate
V_b	Bulk volume of liquid phase
V_c	Total volume of catalyst particles in reactor
γ	Liquid to catalyst volume ratio: $V_b/A \cdot R$ or $V_b/3 \cdot V_c$
η	Effectiveness factor
η'	Overall effectiveness factor
ρ	Dimensionless radius (r/R)
σ	Dimensionless reaction rate
τ	Dimensionless reaction time
Φ	Thiele modulus for Penicillin G
Φ_1	Thiele modulus for PAA
Φ_2	Thiele modulus for APA

Introduction

Enzyme immobilization to solid supports has been a landmark in enzyme biocatalysis because it allows biocatalyst reuse and may increase enzyme stability [1, 2]. These are critical aspects in enzymatic process development that are tightly linked to process

economy. The carrier particles are usually porous with the enzyme immobilized in its internal surface. Both continuous and batch processes can be conducted with immobilized enzymes. The former have potential advantages in terms of productivity and process control; however, continuous packed-bed reactors can suffer from clogging and frequent wash cycles have to be considered, and on the other hand, continuous stirred tank reactors are kinetically disfavored more so if the enzyme is subjected to product inhibition. Therefore, batch reaction has been often used despite its disadvantages, and in the case of immobilized enzymes, operation is done in consecutive batches where the enzyme is recovered after the desired conversion has been attained and used again until the criterion of biocatalyst replacement is met [3]. Recovery of the enzyme can be done in this case simply by sifting, and it is customary to conduct this operation within the reactor to avoid excess handling of the biocatalyst.

According to the theory of diffusional restrictions in enzyme catalysts [4, 5], both the catalytic potential and effectiveness of the enzyme are impaired when mass transfer limitations are present. These effects are caused by diminished concentration of substrate and accumulation of potentially inhibitory products inside the catalyst particle. This has been demonstrated for the hydrolysis of lactose with β-galactosidase, where product inhibition by galactose reduced substrate conversion and decreased the effectiveness factor [6]. Additionally, apparent Michaelis constants were increased in response to the magnitude of internal diffusional restrictions (IDR) [5], which is conveniently expressed by the dimensionless parameter Thiele modulus (Φ), which properly represents the ratio between reaction and diffusion rates. Thiele modulus depends on the kinetic properties of the enzyme: catalytic rate constant and substrate affinity, and on mass transfer properties: effective diffusion of substrate and products and catalyst particle size and geometry [5, 7]. Operational parameters as catalyst enzyme loading, particle size, and substrate concentration are key aspects on process design for proper reactor operation.

Models for enzyme kinetics under diffusional restrictions have been analyzed in previous publications. Al-Muftah and Abu-Reesh studied the effect of external and internal diffusional restrictions on a simulated packed-bed reactor with immobilized enzyme for lactose hydrolysis, concluding that effects of Stanton (*St*) and Peclet (*Pe*) numbers on effectiveness factor have a strong dependence on kinetic parameters [6]. In this work, the effectiveness factor was calculated numerically. Another attempt for evaluating enzyme kinetics under diffusional restrictions was done by Li et al., where a third-order approximate solution valid for quick estimation of substrate distribution and effectiveness factor was developed [8]. A mathematical model for describing the influence of external mass transfer limitations on penicillin G hydrolysis with penicillin G acylase was proposed by Kheirolomoom et al. [9]. This model was used for external mass transfer coefficient ($k_L a$) estimation. A multicomponent reaction–diffusion model for the synthesis of cephalexin with immobilized penicillin acylase heterogeneously distributed in a porous carrier was also reported [10]. Relevant insights in intraparticle process dynamic were revealed considering enzyme distribution, electrostatically coupled transport, pH-dependent dissociation, and pH gradients.

In the present work, the heterogeneous enzymatic catalysis of the reaction of hydrolysis of penicillin G with immobilized penicillin G acylase in a batch reactor is modeled considering two phases: the bulk liquid phase containing the dissolved substrate (penicillin G) and products (phenylacetic acid and 6-aminopenicillanic acid) and the solid biocatalyst phase where the reaction takes place and substrate is converted into products. Biocatalyst particles are suspended in the liquid phase by means of mechanical agitation, which allows the homogeneous distribution of catalyst particles throughout the reactor and may reduce

the magnitude of external (film) diffusional restrictions (EDR). A model was developed considering both the mass transfer of substrate and products between the bulk liquid phase and the solid catalyst and the enzyme catalyzed reaction taking place inside the catalyst particles. The simulated batch reactor operation for the hydrolysis of penicillin G with immobilized penicillin acylase is developed to evaluate the impact of IDR on effectiveness factor and productivity. Modeling and simulation of the hydrolysis of penicillin G in a batch reactor were done to evaluate the impact of two fundamental properties of the biocatalyst, namely enzyme loading and particle size, on specific productivity. Two opposed effects are expected when enzyme loading is increased: increase in reaction rate on one hand and increase in mass transfer limitations on the other; the former will increase productivity while the latter will impair it. When particle size is increased, recovery of catalyst will be easier and less costly, but productivity will be negatively affected by mass transfer limitations. The net effect will depend on the kinetic and mass transfer properties of the system, so it has to be evaluated through a systematic analysis of simulations made from a sound mathematical model describing the reaction system. Valuable information for proper process and biocatalyst design will be obtained from this analysis, being a necessary step towards the technological implementation of the enzyme process.

Model Development

Penicillin acylase (EC 3.5.1.11) is a very versatile enzyme that catalyzes both the hydrolysis of penicillin G and the synthesis of β-lactam antibiotics, such as amoxicillin and cephalexin [11]. Hydrolysis of penicillin G is represented as:

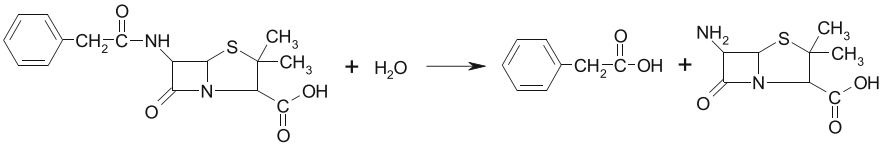

Penicillin G (S) PAA (P_1) APA (P_2)

A rate equation for the hydrolysis of penicillin G has been validated by Kheirolomoom et al. [12]. It involves double product inhibition, being phenylacetic acid (PAA) a competitive inhibitor and (APA) a noncompetitive inhibitor. In addition, inhibition by high substrate concentration is considered. Rate equation is presented in Eq. 1.

$$v = \frac{kES}{K + S + \frac{S^2}{K_S} + \frac{KP_1}{K_1} + \frac{KP_2}{K_2} + \frac{SP_2}{K_2} + \frac{KP_1P_2}{K_1K_2}} \tag{1}$$

The catalyst, which is suspended in the aqueous reaction phase by mechanical agitation, corresponds to penicillin G acylase from *Escherichia coli* immobilized by multipoint covalent attachment to a porous matrix of glyoxyl-agarose spherical particles [1, 2]. Cross-linked 6% agarose spherical beads with a mean bead diameter of 96 μm were considered as catalyst matrix. The kinetic model is based on an ordered sequential mechanism, as previously proposed and validated [12–15]. Mass transfer between catalyst and bulk liquid

phase was modeled by Fick's law. Kinetic parameters in Eq. 1 and effective diffusion coefficients of substrate and products were experimentally determined at 30 °C and pH 7.8 as described in a previous work [16].

The model is constructed from equations that describe the process of diffusion and reaction inside the biocatalyst particles. A flexible system of equations is obtained for spherical biocatalyst particles allowing the simulation of the hydrolysis of penicillin G in batch reactor for the determination of conversion profiles and substrate and products concentration profiles within the catalyst particles. The model is based on substrate and products mass balances within the catalyst, which are decsribed by Eqs. 2, 3, and 4. These are called the reaction–diffusion equations.

$$\frac{\partial S}{\partial t} = D_e\left(\frac{\partial^2 S}{\partial r^2} + \frac{2}{r}\frac{\partial S}{\partial r}\right) - \frac{kES}{K\left[1 + \frac{S}{K} + \frac{S^2}{KK_S} + \frac{P_1}{K_1} + \frac{P_2}{K_2} + \frac{SP_2}{KK_2} + \frac{P_1}{K_1}\frac{P_2}{K_2}\right]} \tag{2}$$

$$\frac{\partial P_1}{\partial t} = D_{e1}\left(\frac{\partial^2 P_1}{\partial r^2} + \frac{2}{r}\frac{\partial P_1}{\partial r}\right) + \frac{kES}{K\left[1 + \frac{S}{K} + \frac{S^2}{KK_S} + \frac{P_1}{K_1} + \frac{P_2}{K_2} + \frac{SP_2}{KK_2} + \frac{P_1}{K_1}\frac{P_2}{K_2}\right]} \tag{3}$$

$$\frac{\partial P_2}{\partial t} = D_{e2}\left(\frac{\partial^2 P_2}{\partial r^2} + \frac{2}{r}\frac{\partial P_2}{\partial r}\right) + \frac{kES}{K\left[1 + \frac{S}{K} + \frac{S^2}{KK_S} + \frac{P_1}{K_1} + \frac{P_2}{K_2} + \frac{SP_2}{KK_2} + \frac{P_1}{K_1}\frac{P_2}{K_2}\right]} \tag{4}$$

Initial conditions for substrate and products are expressed as:

1. Within the catalyst:

$$S(r,0) = P_1(r,0) = P_2(r,0) = 0 \tag{5}$$

2. In the bulk liquid phase and particle surface (r=R):

$$S_{b0} = S(R,0) \tag{6}$$

$$P_{1b0} = P_{2b0} = P_1(R,0) = P_2(R,0) = 0 \tag{7}$$

Boundary conditions on the spherical particle are expressed as:

2. r=0:

$$\left.\frac{\partial S}{\partial r}(r,t)\right|_{r=0} = \left.\frac{\partial P_1}{\partial r}(r,t)\right|_{r=0} = \left.\frac{\partial P_2}{\partial r}(r,t)\right|_{r=0} = 0 \tag{8}$$

2. $r=R$:

$$\left(\frac{\partial S}{\partial r}(r,t)+\frac{V_b}{AD_e}\frac{\partial S}{\partial t}(r,t)\right)\Bigg|_{r=R}=0 \tag{9}$$

$$\left(\frac{\partial P_1}{\partial r}(r,t)+\frac{V_b}{AD_{e1}}\frac{\partial P_1}{\partial t}(r,t)\right)\Bigg|_{r=R}=0 \tag{10}$$

$$\left(\frac{\partial P_2}{\partial r}(r,t)+\frac{V_b}{AD_{e2}}\frac{\partial P_2}{\partial t}(r,t)\right)\Bigg|_{r=R}=0 \tag{11}$$

For all $t>0$, concentration at the catalyst surface ($r=R$) is $S(R,t)=S_b(t)$. This condition considers that EDR are negligible with respect to diffusional restrictions inside catalyst particle, which may be a sound assumption for a well-stirred reactor.

Other assumptions of the model are:

- Constant temperature
- Homogeneous distribution of the enzyme molecules inside the catalyst particle
- Enzyme not affected by thermal inactivation during reaction
- No pH gradients are produced inside catalyst. Constant pH may be reasonably assumed at buffer concentrations above 50 mM [17].

From Eqs. 12, 13, and 14, variations in substrate and products concentration in the bulk liquid phase are obtained:

$$\frac{dS_b}{dt}=-\frac{3D_eV_c}{RV_b}\frac{\partial S}{\partial r}\Bigg|_{r=R} \tag{12}$$

$$\frac{dP_{1b}}{dt}=-\frac{3D_{e1}V_c}{RV_b}\frac{\partial P_{1b}}{\partial r}\Bigg|_{r=R} \tag{13}$$

$$\frac{dP_{2b}}{dt}=-\frac{3D_{e2}V_c}{RV_b}\frac{\partial P_{2b}}{\partial r}\Bigg|_{r=R} \tag{14}$$

Effectiveness factor is defined as the ratio between local reaction rates inside the catalyst particle and reaction rate at surface conditions with bulk substrate and products concentrations:

$$\eta=\frac{v(S(r,t),P_1(r,t),P_2(r,t))}{v(S_b(t),P_{1b}(t),P_{2b}(t))} \tag{15}$$

To evaluate the overall effectiveness factor of the catalyst particle, an integrated mean value is calculated from the distribution of local effectiveness factors inside the catalyst particle:

$$\eta' = \frac{\int_0^R r^2 \eta dr}{\int_0^R r^2 dr} \tag{16}$$

The model is now expressed in dimensionless form, having the advantage that Thiele modulli are obtained for IDR impact evaluation from kinetic and diffusional properties. Computer implementation of mathematical algorithms is also favored when equations are expressed in dimensionless form. The following variables are defined:

Dimensionless time:

$$\tau = t/T \qquad T = R^2/D_e \tag{17}$$

Dimensionless radius:

$$\rho = r/R \tag{18}$$

Dimensionless concentrations:

$$s = S/K, p = P_1/K_1, q = P_2/K_2 \tag{19}$$

Dimensionless rate equation:

$$\sigma = \frac{s}{1 + s + \frac{K}{K_S} s^2 + p + q + sq + pq} \tag{20}$$

Thiele modulli:

$$\Phi = \frac{R}{3}\sqrt{\frac{k \cdot E}{K \cdot D_e}}, \Phi_1 = \frac{R}{3}\sqrt{\frac{k \cdot E}{K_1 \cdot D_{e1}}}, \Phi_2 = \frac{R}{3}\sqrt{\frac{k \cdot E}{K_2 \cdot D_{e2}}} \tag{21}$$

Equations 22, 23, and 24 are the dimensionless forms of Eqs. 2, 3, and 4, respectively:

$$\frac{\partial s}{\partial \tau} = \left(\frac{\partial^2 s}{\partial \rho^2} + \frac{2}{\rho} \cdot \frac{\partial s}{\partial \rho}\right) - 9 \cdot \Phi^2 \sigma \tag{22}$$

$$\frac{\partial p}{\partial \tau} = \frac{D_{e1}}{D_e} \cdot \left(\frac{\partial^2 p}{\partial \rho^2} + \frac{2}{\rho} \cdot \frac{\partial p}{\partial \rho}\right) + 9 \cdot \Phi_1^2 \sigma \tag{23}$$

$$\frac{\partial q}{\partial \tau} = \frac{D_{e2}}{D_e} \cdot \left(\frac{\partial^2 q}{\partial \rho^2} + \frac{2}{\rho} \cdot \frac{\partial q}{\partial \rho}\right) + 9 \cdot \Phi_2^2 \sigma \tag{24}$$

Initial conditions:

1. Within the catalyst:

$$s(\rho,0)=p(\rho,0)=q(\rho,0)=0 \tag{25}$$

2. In the bulk liquid phase and catalyst surface (ρ=1):

$$s(1,0)=s_{b0}=S_{b0}/K \tag{26}$$

$$p_b=q_b=p(1,0)=q(1,0)=0 \tag{27}$$

Boundary conditions:

1. ρ=0:

$$\left.\frac{\partial s}{\partial \rho}(\rho,\tau)\right|_{\rho=0}=\left.\frac{\partial p}{\partial \rho}(\rho,\tau)\right|_{\rho=0}=\left.\frac{\partial q}{\partial \rho}(\rho,\tau)\right|_{\rho=0}=0 \tag{28}$$

2. ρ=1, using notation $\gamma=\frac{V_b}{AR}$:

$$\left.\left(\frac{\partial s}{\partial \rho}(\rho,\tau)+\gamma\frac{\partial s}{\partial \tau}(\rho,\tau)\right)\right|_{\rho=1}=0 \tag{29}$$

$$\left.\left(\frac{\partial p}{\partial \rho}(\rho,\tau)+\frac{D_e}{D_{e1}}\gamma\frac{\partial p}{\partial \tau}(\rho,\tau)\right)\right|_{\rho=1}=0 \tag{30}$$

$$\left.\left(\frac{\partial q}{\partial \rho}(\rho,\tau)+\frac{D_e}{D_{e2}}\gamma\frac{\partial q}{\partial \tau}(\rho,\tau)\right)\right|_{\rho=1}=0 \tag{31}$$

Substrate and products variation in bulk liquid phase during reaction in dimensionless form is:

$$\frac{\partial s_b}{\partial \tau}=-\frac{1}{\gamma}\left.\frac{\partial s}{\partial \rho}\right|_{\rho=1} \tag{32}$$

$$\frac{\partial p_b}{\partial \tau}=-\frac{D_{e1}}{\gamma D_e}\left.\frac{\partial p}{\partial \rho}\right|_{\rho=1} \tag{33}$$

$$\frac{\partial q_b}{\partial \tau}=-\frac{D_{e2}}{\gamma D_e}\left.\frac{\partial q}{\partial \rho}\right|_{\rho=1} \tag{34}$$

In order to perform the simulation of reactor operation, dimensionless Eqs. 22–24, 32–34 and initial and boundary conditions Eqs. 25–31 were discretized through finite differences utilizing the Crank–Nicolson method (see Appendix). Discretized equations were implemented and solved with Python software available in http://www.python.org/. A module was created which documentation, codes, and manual are available in http://www.pypsdier.org/home. Dimensionless Eqs. 22–34 are general expressions for any heterogeneous enzymatic reaction system with spherical catalyst. In this way, the mathematical expressions can be applied to enzymatic systems other than the hydrolysis of penicillin G. In that case, the kinetic expression (σ) has to be adjusted to the corresponding mechanism and the kinetic and diffusion parameters have to be determined for the particular enzyme and reaction system. The number of equations will depend on the number of reactive species (substrates and products). The model developed for hydrolysis of penicillin G can be further improved by including thermal inactivation of the enzyme ($E=f(T,t)$), uneven distribution of the enzyme within the catalyst particle ($E=f(\rho)$) and pH and temperature dependence of the kinetic parameters ($K_i=f(pH, T)$).

Time course of penicillin G conversion was obtained from simulation of batch reactor. Conversion was defined as the mass of hydrolyzed penicillin G per unit mass of initial penicillin G. Volumetric productivity (amount of hydrolyzed penicillin G per unit time and unit of reaction volume) was calculated at 95% conversion:

$$Q_p = \frac{213 \cdot S_{b0} \cdot 0.95}{t_{0.95}} \left(\mathrm{gAPA/l \cdot h}\right) \tag{35}$$

Specific productivity was obtained by dividing the volumetric productivity by the reactor enzyme concentration (E_R) corresponding to the total enzyme activity loaded to the batch reactor:

$$Q_{pe} = \frac{Q_p}{E_R} \left(\mathrm{gAPA/h \cdot IU}\right) \tag{36}$$

One international unit (IU) of penicillin G acylase was defined as the quantity of enzyme that hydrolyzes 1 μmol of penicillin per minute. The amount of enzyme used in the batch reactor was calculated from the catalyst enzyme loading (IU per unit mass of catalyst) and catalyst mass in the reactor.

Table 1 Kinetic and diffusion parameters for penicillin G hydrolysis model

Substance	Parameter	Value	Units
Enzyme	k	43	1/s
Penicillin G	K	0.13	mM
Penicillin G	K_S	821	mM
PAA	K_1	1.82	mM
APA	K_2	48	mM
Penicillin G	D_e	$5.30 \cdot 10^{-10}$	m^2/s
PAA	D_{e1}	$7.33 \cdot 10^{-10}$	m^2/s
APA	D_{e2}	$5.89 \cdot 10^{-10}$	m^2/s

Results and Discussion

Experimentally determined kinetic and diffusion parameters used in the simulations are reproduced in Table 1 [16]. From these values, it is possible to calculate the Thiele modulus values for penicillin G, PAA, and APA by means of Eq. 21. Penicillin G modulus is higher than those for the products because of the small value of K as compared to K_1 and K_2. From these three Thiele moduli, the one for penicillin G represents a diffusional restriction parameter for the proper characterization of mass transfer limitations in the hydrolysis reaction because K represents the affinity of the enzyme for its substrate being a determinant of the reaction rate.

Concentration Profiles Inside the Catalyst Particles

One of the interesting features of simulations in heterogeneous catalysis is the possibility to analyze concentration profiles inside the catalyst. This is a hardly observable phenomenon that can be described by simulation evidencing the impact of mass transfer limitations. Substrate and products concentrations are calculated by Eqs. 22–24 and depend on catalyst particle size, effective diffusion, and reaction rates. Combination of these properties allows the determination of the concentration profiles inside the catalyst particles. Figures 1 and 2 show the concentration profiles of penicillin G, PAA, and APA inside the catalyst during the reaction of hydrolysis in batch reactor. Diffusional restrictions cause substrate depletion and products accumulation towards the center of particle. Substrate and product profiles revealed the existence of IDR throughout the reaction time. Accumulation of products increases enzyme inhibition, adding to the effect of diffusional restrictions in reducing the catalytic potential of the biocatalyst.

The effect of the difference in effective diffusion coefficients between PAA and APA can be appreciated in Fig. 2. APA diffuses more slowly than PAA, so its accumulation inside the catalyst is higher. Nevertheless, no differences are obtained on the catalyst surface and in the bulk liquid phase.

Reaction rates within the catalyst particle are lower than those at the biocatalyst surface. Overall effectiveness factor allows the quantification of this phenomenon. It depends on the Thiele modulus and substrate concentration in the bulk liquid phase. As concentrations vary with time, overall effectiveness factor does too and, as seen above, the catalytic potential of the enzyme is reduced not only by diffusional restrictions but also because of the dual product inhibition. Overall effectiveness factors as a function of time are shown in Fig. 3, with Thiele modulus and substrate concentration as parameters.

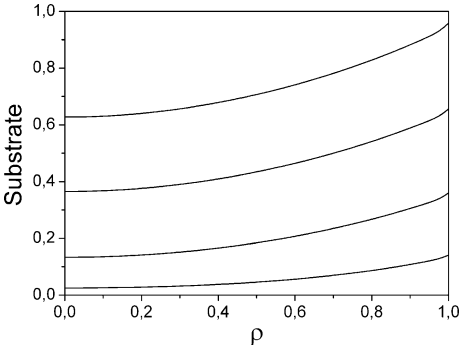

Fig. 1 Dimensionless penicillin G concentration profiles inside catalyst particle in batch reactor at reactiontimes of 10, 100, 200, and 300 s and corresponding conversions of 0.04, 0.34, 0.64, and 0.86. Initial penicillin G concentration: 13 mM; enzyme concentration in reactor: 3 IU/ml; Thiele modulus=5

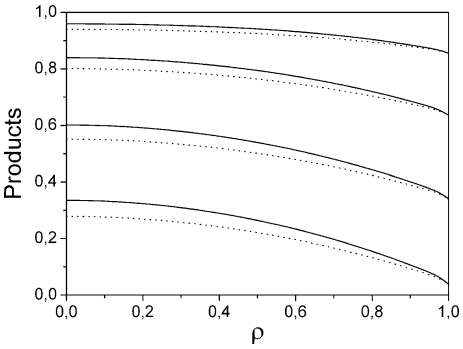

Fig. 2 Dimensionless PAA (*dotted line*) and APA (*solid line*) concentration profiles inside catalyst particle in batch reactor at reaction times of 10, 100, 200, and 300 s and corresponding conversions of 0.04, 0.34, 0.64, and 0.86 in batch reactor. Initial penicillin G concentration: 13 mM; enzyme concentration in reactor: 3 IU/ml; Thiele modulus=5

Overall effectiveness factor is highly dependent on internal diffusional restrictions at low penicillin G concentrations. On the other hand, high concentrations reduce the diffusional restrictions significantly with near unit even at high values of Thiele modulus. Overall effectiveness factor diminishes with time because of substrate consumption. This effect is buffered at high initial concentrations of penicillin G. Nevertheless, at high conversion and high values of Thiele modulus, overall effectiveness factor decay anyway, reducing productivity. Effect of substrate inhibition is mild a high initial concentration of penicillin G, as noted in Fig. 3d. This is due to the high value of the substrate inhibition constant (K_S=821 mM). For proper characterization of diffusional restrictions, overall effectiveness factors at different substrate conversions have been correlated with the operational parameters Thiele modulus and initial substrate concentration in Fig. 4.

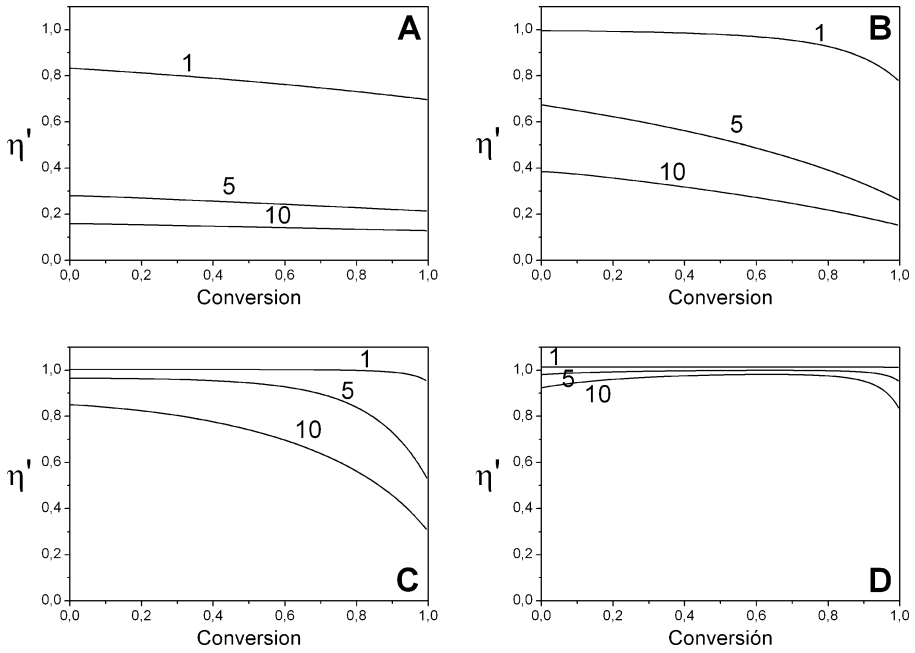

Fig. 3 Overall effectiveness factor as a function of reaction time (substrate conversion) during the hydrolysis of penicillin G in batch reactor for different values of Thiele modulus (Φ=1, 5, 10) and initial dimensionless penicillin G concentrations: 1 (**a**), 10 (**b**), 100 (**c**), and 1,000 (**d**). Enzyme concentration in reactor: 3 IU/ml

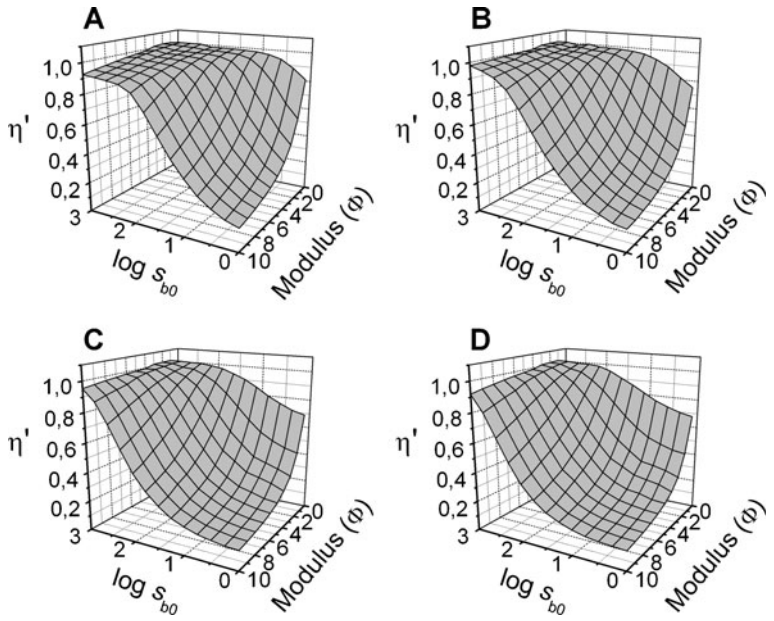

Fig. 4 Overall effectiveness factor (η') as a function of Thiele modulus for penicillin G (Φ) and dimensionless bulk penicillin G concentration (s_{b0}) for the hydrolysis of penicillin G with immobilized penicillin acylase catalysts at the beginning of the reaction (**a**) and at substrate conversion 0.5 (**b**), 0.9 (**c**), and 0.95 (**d**)

Batch Reactor Performance

Batch reactor performance is obtained from conversion curves of penicillin G in bulk liquid phase. Variation in penicillin G, PAA and APA concentrations through time is modeled by Eqs. 32–34 which now depend on catalyst performance and mass transfer, as represented by Eqs. 22–24. Reactor performance in terms of conversion versus time at varying initial substrate concentrations and Thiele modulus and at equal reactor enzyme concentrations is presented in Fig. 5. This reflects the impact of diffusional restrictions on reactor performance because the same amount of enzyme is loaded in the reactor in each case. Diffusional restrictions affect reactor performance by diminishing reaction rate, which implies that higher times will be required to attain a certain level of conversion. Consequently, productivity is impaired. As it occurs with the effectiveness factor, differences between operational curves at different values of the Thiele modulus are minimized at high substrate concentrations.

Volumetric productivity was calculated from operational curves at 95% conversion, as stated in Eq. 35. This is dependent on the amount of enzyme used in the reactor, for the higher it is, the higher the volumetric productivity obtained. Specific productivity is defined as a response variable independent of the amount of enzyme in the reactor. In addition, it is a cost-effective parameter in reactor operation. Figure 6 presents the specific productivity in terms of APA production.

A maximum value of specific productivity is observed with respect to initial penicillin G concentration. This is due to noncompetitive product inhibition by APA. Competitive inhibition by PAA is counteracted at high penicillin G concentrations; however,

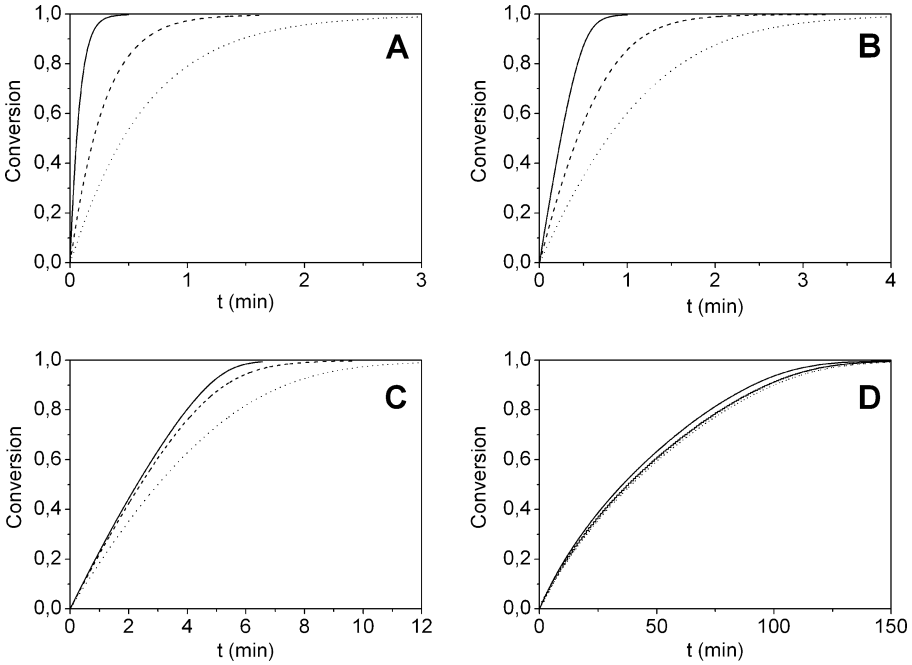

Fig. 5 Reactor performance for penicillin G hydrolysis in batch reactor for different initial penicillin G concentrations and values of Thiele modulus 1 (*solid line*), 5 (*dashed line*), and 10 (*dotted line*). Dimensionless penicillin G concentration (s_{b0}): 1 (**a**), 10 (**b**), 100 (**c**), 1,000 (**d**). Enzyme concentration in reactor: 3 UI/ml

noncompetitive inhibition by APA is not, since the decrease in apparent V_{max} is independent of penicillin G concentration. The specific productivity is a very convenient cost–gain function as it contains productivity of 6-APA (gain) and enzyme used in reactor (cost). The result is not obvious because the net result will stem from the combination of the kinetic and mass transfer properties of the system. To obtain a higher productivity, catalyst enzyme loading must be increased, but specific productivity is not necessarily enhanced, as

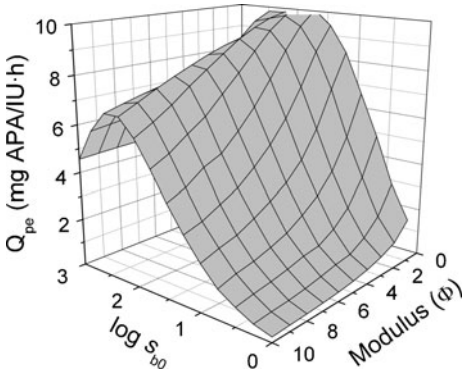

Fig. 6 Specific productivity with respect to APA for penicillin G hydrolysis in batch reactor at different values of Thiele modulus and penicillin G initial concentration

seen in Fig. 6, as well as process profitability. The maximum specific productivity is obtained at a penicillin G concentration of approximately 100 mM, maybe not quite convenient for the downstream operations. So, higher initial concentrations of penicillin G could be preferable even at the expense of lower specific productivities.

The same kind of analysis is needed when the proper catalyst particle size has to be chosen. In this case, the recovery of the catalyst is easier and less costly for bigger particle sizes. Nevertheless, bigger sizes imply increased mass transfer limitations, reduced specific productivity and a worse cost–gain relationship. The following is an analysis of the particle size effect on specific productivity. Thiele modulus contains two very important catalyst operational parameters: enzyme loading and particle size, the latter having a stronger effect over the overall effectiveness and productivity. A batch reactor operating with a catalyst with a specific activity of 400 IU/g_{cat} was considered to evaluate the effect of particle size on specific productivity. This enzyme loading is relatively high with respect to values reported in the literature [17, 18]. Penicillin G concentration for the industrial production of APA range from 180 to 260 mM [19]. The value of 260 mM was chosen being 2,000 times larger than the value of *K*. Catalyst particle sizes between 25 and 1,000 μm were considered. Results are presented in Fig. 7. A twofold difference in specific productivity is obtained with catalysts of 25 and 1,000 μm in radius. This is a significant and enlightening result for proper process design.

Catalyst enzyme loading and particle size affect significantly the specific productivity, being important operational variables for process optimization and technological profitability. The catalyst for penicillin G hydrolysis must be selected in terms of enzyme loading and particle size taking into account their impact on productivity, as a cost–gain function but also the costs associated to the enzyme and catalyst recovery.

Conclusions

A mathematical model based on enzyme kinetics and mass transfer was developed as a tool for the proper analysis of the effect of operational parameters on reactor performance in the reaction of hydrolysis of penicillin with immobilized penicillin acylase. Increasing diffusional restrictions, as a consequence of increasing enzyme loading and particle size, decreased productivity. On the other hand, increased penicillin G concentration reduced the impact of diffusional restrictions but increased the impact

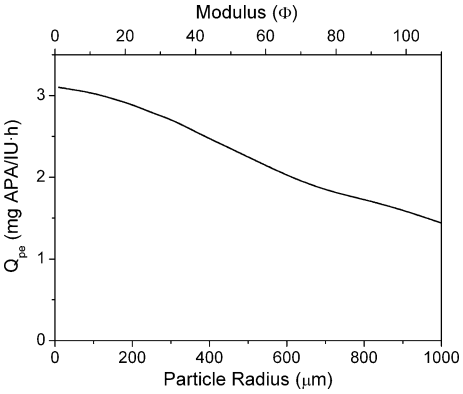

Fig. 7 Specific productivity with respect to APA for the hydrolysis of penicillin G in batch reactor as a function of particle size. Initial dimensionless penicillin G concentration was 260 mM. Specific activity of the catalyst was 400 IU/g

of product inhibition. The net effect obtained from this model is a nonlinear relationship between catalyst enzyme loading and specific productivity, which implies that an increase in the amount of enzyme will not increase the volumetric productivity by the same magnitude as it occurs with a soluble enzyme where no diffusional restrictions exists. In the case of biocatalyst particle size, results indicate that its increase has always a negative effect on specific productivity so that catalyst recovery costs have to be included in the analysis to determine the best particle size. The performance of immobilized penicillin G acylase catalysts in the batch reaction of hydrolysis of penicillin G for APA production is governed by particle size, enzyme loading, and initial penicillin G concentration. The analysis of the effect of these three parameters in reactor performance is a key aspect for process optimization.

Acknowledgements Work funded by Chilean Fondecyt Project 1080122.

Appendix

Simulation was done by solving Eqs. 22–24 and 32–34. Dimensionless equations were discretized using Crank–Nicolson method to achieve stability during solution processing in computer programs. The number of equations depends on N obtaining $N+1$ equations for each substance. In this study, $N=20$ was used obtaining a system of 63 equations. Algebraic form of discretized equations are as follows:

For $j=0$:

$$-\frac{3}{2}s_0 + 2s_1 - \frac{1}{2}s_2 = 0$$

$$-\frac{3}{2}p_0 + 2p_1 - \frac{1}{2}p_2 = 0$$

$$-\frac{3}{2}q_0 + 2q_1 - \frac{1}{2}q_2 = 0$$

For $j=1,\ldots, N-1$:

$$s_j^{n+1} - \frac{\Delta\tau}{2(\Delta\rho)^2}\left(\left[1-\frac{1}{j}\right]s_{j-1}^{n+1} - 2s_j^{n+1} + \left[1+\frac{1}{j}\right]s_{j+1}^{n+1}\right) = s_j^n + \frac{\Delta\tau}{2(\Delta\rho)^2}\left(\left[1-\frac{1}{j}\right]s_{j-1}^{n} - 2s_j^{n} + \left[1+\frac{1}{j}\right]s_{j+1}^{n}\right) - \Delta\tau\Phi^2\sigma_j^n$$

$$p_j^{n+1} - \frac{D_{e1}\Delta\tau}{2(\Delta\rho)^2}\left(\left[1-\frac{1}{j}\right]p_{j-1}^{n+1} - 2p_j^{n+1} + \left[1+\frac{1}{j}\right]p_{j+1}^{n+1}\right) = p_j^n + \frac{D_{e1}\Delta\tau}{2(\Delta\rho)^2}\left(\left[1-\frac{1}{j}\right]p_{j-1}^{n} - 2p_j^{n} + \left[1+\frac{1}{j}\right]p_{j+1}^{n}\right) - \Delta\tau\Phi_1^2\sigma_j^n$$

$$q_j^{n+1} - \frac{D_{e2}\Delta\tau}{2(\Delta\rho)^2}\left(\left[1-\frac{1}{j}\right]q_{j-1}^{n+1} - 2q_j^{n+1} + \left[1+\frac{1}{j}\right]q_{j+1}^{n+1}\right)$$
$$= q_j^n + \frac{D_{e2}\Delta\tau}{2(\Delta\rho)^2}\left(\left[1-\frac{1}{j}\right]q_{j-1}^n - 2q_j^n + \left[1+\frac{1}{j}\right]q_{j+1}^n\right) - \Delta\tau\Phi_2^2\sigma_j^n$$

For $j = N$:

$$s_N^{n+1} + \frac{\Delta\tau}{2\gamma\Delta\rho}\left(-\frac{1}{2}s_{N-2}^{n+1} + 2s_{N-1}^{n+1} - \frac{3}{2}s_N^{n+1}\right) = s_N^n - \frac{\Delta\tau}{2\gamma\Delta\rho}\left(-\frac{1}{2}s_{N-2}^n + 2s_{N-1}^n - \frac{3}{2}s_N^n\right)$$

$$p_N^{n+1} + \frac{D_{e1}\Delta\tau}{2\gamma\Delta\rho}\left(-\frac{1}{2}p_{N-2}^{n+1} + 2p_{N-1}^{n+1} - \frac{3}{2}p_N^{n+1}\right)$$
$$= p_N^n - \frac{D_{e1}\Delta\tau}{2\gamma\Delta\rho}\left(-\frac{1}{2}p_{N-2}^n + 2p_{N-1}^n - \frac{3}{2}p_N^n\right)$$

$$q_N^{n+1} + \frac{D_{e2}\Delta\tau}{2\gamma\Delta\rho}\left(-\frac{1}{2}q_{N-2}^{n+1} + 2q_{N-1}^{n+1} - \frac{3}{2}q_N^{n+1}\right)$$
$$= q_N^n - \frac{D_{e2}\Delta\tau}{2\gamma\Delta\rho}\left(-\frac{1}{2}q_{N-2}^n + 2q_{N-1}^n - \frac{3}{2}q_N^n\right)$$

References

1. Mateo, C., Abián, O., Bernedo, M., Cuenca, E., Fuentes, M., Fernández-Lorente, G., et al. (2005). *Enzyme and Microbial Technology, 37*, 456–462.
2. Mateo, C., Palomo, J. M., Fuentes, M., Betancor, L., Grazu, V., López-Gallego, F., et al. (2006). *Enzyme and Microbial Technology, 39*, 274–280.
3. Illanes, A., & Wilson, L. (2003). *Critical Reviews in Biotechnology, 23*, 61–93.
4. Shuler, M., Aris, R., & Tsuchiya, H. (1972). *Journal of Theoretical Biology, 35*, 67–76.
5. Engasser, J., & Horvath, C. (1973). *Journal of Theoretical Biology, 42*, 137–155.
6. Al-Muftah, A., & Abu-Reesh, I. (2005). *Biochemical Engineering Journal, 23*, 139–153.
7. Illanes, A. (2008). *Enzyme biocatalysis: Principles and applications*. London: Springer.
8. Li, X., Chen, X., & Chen, N. (2004). *Biochemical Engineering Journal, 17*, 65–69.
9. Kheirolomoom, A., Khorasheh, F., & Fazelinia, H. (2002). *Journal of Bioscience and Bioengineering, 93*, 125–129.
10. Van Roon, J. L., Arntz, M. M. H. D., Kallenberg, A. I., x Paasman, A. I., Tramper, J., Schroën, C. G. H. P., et al. (2006). *Applied Microbiology and Biotechnology, 72*, 263–278.
11. Illanes, A., & Wilson, L. (2006). *Chimica Oggi/Chemicals Today, 24*, 27–30.
12. Kheirolomoom, A., Ardjmand, M., Fazelinia, H., & Zakeri, A. (2001). *Process Biochemistry, 36*, 1095–1101.
13. Balasingham, K., Warburton, D., Dunill, P., & Lilly, M. D. (1972). *Biochimica et Biophysica Acta Enzymology, 276*, 250–256.
14. Warburton, D., Dunnill, P., & Lilly, M. (1973). *Biotechnology and Bioengineering, 15*, 13–25.
15. Lee, S. B., & Ryu, D. (1982). *Enzyme and Microbial Technology, 4*, 35–38.
16. Valencia, P., Flores, S., Wilson, L., & Illanes, A. (2010). *Biochemical Engineering Journal, 49*, 256–263.
17. Guisán, J. M., Alvaro, G., Rosell, C., & Fernandez-Lafuente, R. (1994). *Biotechnology and Applied Biochemistry, 20*, 357–369.
18. Ospina, S., López-Mungia, A., González, R., & Quintero, R. (1992). *Journal of Chemical Technology and Biotechnology, 53*, 205–213.
19. Shewale, J., & Sivaraman, H. (1989). *Process Biochemistry, 24*, 146–154.